Acta Crystallographica Section A
Foundations of Crystallography
ISSN 0108-7673

Received 11 September 2009
Accepted 28 October 2009

The long-wavelength limit of the structure factor of amorphous silicon and vitreous silica

Adam M. R. de Graff and M. F. Thorpe*

Physics Department, Arizona State University, Tempe, AZ 85287, USA. Correspondence e-mail: mft@asu.edu

Liquids are in thermal equilibrium and have a non-zero structure factor $S(Q \rightarrow 0) = [\langle N^2\rangle - \langle N\rangle^2]/\langle N\rangle = \rho_0 k_B T \chi_T$ in the long-wavelength limit where ρ_0 is the number density, T is the temperature, Q is the scattering vector and χ_T is the isothermal compressibility. The first part of this result involving the number N (or density) fluctuations is a purely geometrical result and does not involve any assumptions about thermal equilibrium or ergodicity, so is obeyed by all materials. From a large computer model of amorphous silicon, local number fluctuations extrapolate to give $S(0) = 0.035 \pm 0.001$. The same computation on a large model of vitreous silica using only the silicon atoms and rescaling the distances gives $S(0) = 0.039 \pm 0.001$, which suggests that this numerical result is robust and perhaps similar for all amorphous tetrahedral networks. For vitreous silica, it is found that $S(0) = 0.116 \pm 0.003$, close to the experimental value of $S(0) = 0.0900 \pm 0.0048$ obtained recently by small-angle neutron scattering. Further experimental and modeling studies are needed to determine the relationship between the fictive temperature and structure.

1. Introduction

Correlated density fluctuations over large length scales can be determined from the small Q limit of the structure factor $S(Q)$, and thus can be obtained directly from diffraction experiments (Egami & Billinge, 2003). The structure factor can be defined in terms of the real-space pair density $\rho(r)$ *via* the sine Fourier transform

$$Q[S(Q) - 1] = \int_0^\infty 4\pi r[\rho(r) - \rho_0] \sin Qr \, dr = \int_0^\infty G(r) \sin Qr \, dr, \quad (1)$$

where ρ_0 is the average density and $G(r) = 4\pi r[\rho(r) - \rho_0]$ is the pair distribution function. This is also a convenient way to obtain $S(Q)$ from computer-generated structural models, as $\rho(r)$ and hence $G(r)$ is rather straightforward to compute.

Of interest here is the structure factor (Egami & Billinge, 2003) in the small Q (corresponding to large distance) limit, $S(Q \rightarrow 0)$, which has rarely been discussed in the context of amorphous modeling but which is actually of considerable interest. We will refer to this limit as the long-wavelength limit of the structure factor, which can be measured by small-angle elastic scattering (*i.e.* diffraction) experiments using either X-rays or neutrons; it is of significance theoretically as it contains information about how far the system is from thermal equilibrium, which will be discussed later. In order to obtain any kind of reliable estimate of $S(0)$ from computer-generated models, it is necessary for the model to be large, and in this paper we focus on the large models of amorphous silicon and vitreous silica developed by Mousseau, Barkema and Vink (Vink *et al.*, 2001; Vink & Barkema, 2003), from which we will show that a reliable estimate for $S(0)$ can be extracted.

From general considerations (Hansen & McDonald, 1986), there is a sum rule relating the limit $S(Q \rightarrow 0)$ to the variance in the number of atoms N within a volume V, namely

$$S(0) = \left[\langle N^2\rangle - \langle N\rangle^2\right]/\langle N\rangle \quad (2)$$

in the thermodynamic limit as $V \rightarrow \infty$. In this paper, we demonstrate that the structure factor in the small Q limit is small but non-zero for realistic and large enough models of amorphous silicon and vitreous silica so that numerical values can be obtained with some confidence. For crystals, with no variance in the density owing to their periodicity, equation (2) gives $S(0) = 0$. Note that there are no assumptions about thermal equilibrium in the derivation of (2), which is of purely geometrical origin (Torquato & Stillinger, 2003).

If further assumptions about thermal equilibrium and ergodicity are made, there is the additional result, well known in liquid theory (Hansen & McDonald, 1986), that relates number fluctuations to the isothermal compressibility χ_T, namely

$$\left[\langle N^2\rangle - \langle N\rangle^2\right]/\langle N\rangle = \rho_0 k_B T \chi_T. \quad (3)$$

This relation assumes that all the states of a system at temperature T governed by a potential are sampled according to Boltzmann statistics. Hence for liquids (and other thermodynamic ergodic systems in thermal equilibrium), we have

$$S(0) = \rho_0 k_B T \chi_T. \quad (4)$$

Equation (4) is also true for multi-component chemically ordered systems if ρ_0 is interpreted as the atomic number density and $S(0) = S_{NN}(0)$ is a Bhatia–Thornton structure factor (Bhatia & Thornton, 1970; Salmon, 2006, 2007), where N refers to the number of atoms (although see the caveat about this in §3).

1.1. Amorphous materials

Amorphous silicon is perhaps the furthest from equilibrium of all non-crystalline materials. This is because it is highly strained, with most of the strain being taken up by deviations of the bond angles from their ideal tetrahedral value of 109.5°. Each silicon atom has three degrees of freedom. The important terms in the potential are the bond stretching and angle bending forces around each atom. There are four covalent bonds at each silicon atom, each of which is shared, giving a net of two bond stretching constraints per atom. Of the six angles at each silicon atom, five are independent, giving a total of seven constraints per atom. As there are considerably more constraints than degrees of freedom, the network is highly over-constrained (Thorpe, 1983). In thermal equilibrium, silicon cycles between crystalline solid and liquid forms. There is no glass transition. However, amorphous silicon can be prepared by various techniques involving very fast cooling and provides an extreme example of a non-equilibrium state.

Vitreous silica is a bulk glass, which contains very little strain, as can be seen as follows. The important constraints are the bond stretching and angle bending forces associated with the silicon atoms, as in amorphous silicon. The angular forces at the oxygen ions are weak (Sartbaeva *et al.*, 2006). The total number of constraints per SiO_2 unit is four Si—O bond stretching constraints plus five angular forces at the Si giving a total of nine constraints. However, the number of degrees of freedom per SiO_2 is also nine (three per atom). The system is therefore isostatic and not over-constrained (Thorpe, 1983). Thus, the strong Si—O bond stretching and O—Si—O angle bending forces are well accommodated (although the much weaker Si—O—Si bond stretching force not so), so that vitreous silica is closer to thermal equilibrium than amorphous silicon, although not close enough that equation (4) can be used. However, equation (4) is much more likely to be obeyed if the fictive temperature T_f at which the glass was formed is used instead of T (including for the compressibility). A much slower decrease in $S(0)$ is observed as the temperature is decreased below T_f owing to the freezing out of thermal vibrations about a fixed topology, as shown in the extensive and informative experiments of Levelut *et al.* (Levelut *et al.*, 2002, 2005, 2007), which we discuss in §4.

1.2. Computer models

There are a number of high-quality periodic computer-generated models for amorphous silicon. The first set of coordinates is from a small model with 4096 atoms (henceforth called the 4096 atom model) (Djordjevic *et al.*, 1995), built within a cubic super-cell with sides of length $L = 43.42$ Å. The average bond length is $a = 2.35$ Å, equal to the known value for crystalline silicon, and the model has the same density as crystalline silicon, which is about right for structurally good samples of amorphous silicon containing few voids, defects *etc.* The network was constructed using the Wooten–Winer–Weaire (WWW) technique (Wooten *et al.*, 1985; Djordjevic *et al.*, 1995), based on locally restructuring the topology of crystalline silicon, while keeping the number of atoms and covalent bonds fixed, until the ring statistics settle down and there are no Bragg peaks apparent in the diffraction pattern.

The second model contains 100 000 atoms (referred to as the 100K model) within a cubic super-cell of side $L = 124.05$ Å, with an average bond length of $a = 2.31$ Å, and was built using a modified WWW technique (Vink *et al.*, 2001) based on previous work by Barkema & Mousseau (2000). We note that the models of Barkema & Mousseau have the narrowest angular variance ($\sim 9°$) at the silicon atoms ever achieved in a non-crystalline tetrahedral network, and they also avoid the issue of possible crystal memory effects in WWW-type models as they use a non-crystalline atomic arrangement initially. The 100K model, like other models built by Barkema & Mousseau (2000), has a density $\sim 5\%$ above that of crystalline silicon and void-free amorphous silicon. The reason why this model has a higher density is not entirely clear, but it may be necessary to let the angular variance increase back up to $\sim 11°$ in order to obtain the experimental density of amorphous silicon. The correlation between this angular spread and the density needs further study. The increase in density may also perhaps be caused by the Keating potential used not being quite up to this level of sophistication. This difference should not affect the limit $S(Q \rightarrow 0)$ to first order, as a uniform isotropic compression or expansion of the whole structure leaves the relative number of fluctuations invariant in the thermodynamic limit.

A very large model of vitreous silica (300K model) has been produced by the same group (Vink & Barkema, 2003) by first decorating the 100K amorphous silicon model with an oxygen ion between pairs of silicon ions and relaxing appropriately. With only a few exceptions, all silicon atoms maintain only oxygen atoms as covalently bonded neighbors and *vice versa*. An important difference between the 100K amorphous silicon and the 300K vitreous silica models is that, by effectively changing the fundamental unit from a silicon atom to a corner-sharing SiO_2 tetrahedron, the system is no longer over-constrained but instead isostatic (Thorpe, 1983), a point that was discussed in §1.1. One might expect the greater number of degrees of freedom and the lower internal stress of the vitreous silica model to affect the structure factor, as vitreous silica is much closer than amorphous silicon to being in thermal equilibrium. We will return to this point later.

2. Calculation of the structure factor in the limit $Q \rightarrow 0$

2.1. Directly from the set of pair separations

The structure factor $S(Q)$ can be calculated in a number of ways, some of which are more useful (*i.e.* smoother) than others when extrapolating to $Q \rightarrow 0$. We focus first on

amorphous silicon, a material with a single atomic species. The structure factor can be computed directly from the set of atom coordinates by taking the spherical average of

$$S(Q) = 1 + \frac{1}{N\langle f\rangle^2}\sum_{j\neq k} f_k^* f_j \exp(i\mathbf{Q}\cdot\mathbf{r}_{jk}), \quad (5)$$

where f_j is the scattering factor of atom j. A spherical average yields

$$S(Q) = 1 + \frac{1}{N\langle f\rangle^2}\sum_{j\neq k} f_k^* f_j \frac{\sin Qr_{jk}}{Qr_{jk}}, \quad (6)$$

where the sum $j \neq k$ goes over all pairs of atoms (excluding the self terms) in the periodic cubic super-cell of size L, and is evaluated at $Q_{lmn} = (2\pi/L)(l^2 + m^2 + n^2)^{1/2}$ where l, m and n are integers. Here $\langle f\rangle$ is the average scattering factor.

The computational approach using (6) suffers from two problems. The first is that there are of order N^2 terms in the sum, which becomes somewhat computationally demanding for large models. Second, and more importantly, there are finite size effects at small Q, even with periodic boundary conditions, creating a peak in $S(Q)$ at the origin of finite width $\sim 1/L$ and amplitude N. The peak at small Q, studied by small-angle X-ray or neutron scattering, is given by the convolution of the δ function that would exist at the origin if the model were infinite with a function related to the shape of the box in which the model exists (Lei *et al.*, 2009). This problem at small Q could in principle be alleviated by subtracting the peak at the origin owing to the finite size of the model (or sample), where the form of the peak is known algebraically for a limited set of shapes (Lei *et al.*, 2009; Goodisman, 1980; Goodisman & Coppa, 1981; Kodama *et al.*, 2006) and can be determined numerically for others. The numerical subtraction of two large numbers $O(N)$ would lead to errors of $O(1)$, which is the order of the answer required. A better approach to finding $S(Q)$ in a form suitable for extrapolation to small Q is described below. We note that it is $S(Q)$ in the limit as $Q \rightarrow 0$ that is of interest, and not $S(0)$ itself, as $Q = 0$ is a singular point.

2.2. Fourier transform approach

As a way to circumvent issues associated with the finite size of the sample that affect small Q, the structure factor $S(Q)$ can be obtained from $G(r)$ *via* the sine Fourier transform given in (1). It appears from the form of (1) as though the limit $S(Q \rightarrow 0)$ depends upon the sine transform of $G(r)$ alone, and thus the behavior of $G(r)$ at large r does not contribute much to the limit $S(Q \rightarrow 0)$ [see Fig. 2 for an example of $G(r)$]. This can be shown to be false by expanding (1) in powers of Q and keeping only the lowest-order terms that would dominate in the small Q limit. To the lowest order in Q,

$$S(0) = 1 + \int_0^\infty 4\pi r^2\big[\rho(r) - \rho_0\big]\,\mathrm{d}r = 1 + \int_0^\infty rG(r)\,\mathrm{d}r, \quad (7)$$

which depends on the integral of $rG(r)$, not $G(r)$. This additional factor of r increases the sensitivity of $S(Q \rightarrow 0)$ to the details of the decay in $G(r)$ at large distances. Oscillations in $G(r)$ associated with a single reference atom are known to persist out to large distances (Levashov *et al.*, 2005) and are a serious concern when computing $S(Q \rightarrow 0)$ from a model. In practice, the use of (7) to find the limit $S(Q \rightarrow 0)$ also suffers from poor convergence, although it is superior to using (6).

2.3. Sampling volume method

Quite generally, even in the absence of thermal equilibrium, the small Q limit $S(Q \rightarrow 0)$ is related in the thermodynamic limit to number (or density) fluctuations within sub-regions of volume V according to (2). As we only have models of finite size, even with periodic boundary conditions it is not possible to determine the limit directly and it is necessary to extrapolate to the $N \rightarrow \infty$ limit as best we can. The approach of extrapolating $S(Q)$ as $Q \rightarrow 0$ suffers from finite size effects that cause oscillations about the ideal $S(Q)$ which would be obtained for an infinite model. It is difficult to disentangle the finite size effects from the underlying ideal $S(Q)$, making accurate extrapolation always challenging.

A more accurate determination of $S(Q \rightarrow 0)$ can be achieved through (2). The equality states that the relative variance in the number of atoms within an ensemble of randomly placed bounded convex volumes (Torquato & Stillinger, 2003) is equal to $S(0)$ in the limit that the sampling volume goes to infinity. For a finite sampling volume of fixed shape, the variance in the number of atoms within the enclosed volume, which samples all possible positions and orientations equally, can be divided into terms that scale as the volume, those that scale as the surface area, and those with lower-order dependencies on the length scale of the enclosed volume (Torquato & Stillinger, 2003). If R describes such a sampling length scale, then the relative variance, which divides the variance by the average number of atoms within the sampling volume, can be expressed as the sum of a volume term of order R^0, a surface term of order R^{-1}, and higher-order terms. It is the volume term that is the primary focus here.

Atomic structures for which the number variance does not depend on volume are called hyperuniform, examples of which are materials with a periodic lattice, as their unit cells have well defined volume and density. The number variance for such systems is related to the Gauss circle problem (Bleher *et al.*, 1993; Torquato & Stillinger, 2003; Levashov *et al.*, 2005). The structure factor for crystals is zero, as the structure factor $S(Q)$ is zero for all values of Q smaller than that associated with the first Bragg peak, leading to the result $S(Q \rightarrow 0) = 0$. Also the relative variance of the number fluctuations is clearly zero on length scales that are much greater than the size of the unit super-cell. This result is only strictly true in the absence of diffuse scattering at a temperature of absolute zero, with no zero-point motion *etc*. Note that it is important to take the limit $Q \rightarrow 0$ so as to avoid the singularity at the origin. For all periodic models at large enough length scales (corresponding to small enough Q), the structure factor will go to zero as the long-wavelength limit is approached, owing to the hyperuniformity associated with the crystallinity. Nevertheless we can obtain meaningful results if we restrict ourselves to

distances less than the size of the super-cell and Q values that are small ($\sim 1/L$, where L is the linear dimension of the supercell) but not too small.

For non-crystalline systems, like amorphous silicon and vitreous silica, we will show that determining the relative variance of $N(R)$ for various sampling radii R and extrapolating the result as $R \rightarrow \infty$ provides a much more precise method of extracting the limit $S(Q \rightarrow 0)$ from a finite model. Indeed it is the optimal procedure. The relative variance has been thoroughly described by Torquato & Stillinger (2003) and equation (58) from their paper can be written for spherical sampling volumes as

$$\frac{\langle N(R)^2\rangle - \langle N(R)\rangle^2}{\langle N(R)\rangle} = 1 - \rho_0 \frac{4\pi}{3} R^3 + \frac{1}{n}\sum_{i\neq j}^{n} \alpha(r_{ij}; R), \qquad (8)$$

where n is the number of atoms in the model, and the function $\alpha(r_{ij}; R)$ is the fractional intersection volume of two (continuum) spheres, with radii R and centers separated by r_{ij}. The function $\alpha(r_{ij}; R)$ is proportional to the probability of two points, separated by r_{ij}, both being contained within a randomly placed sphere of radius R, and has a form given by Torquato & Stillinger (2003) in equation (A11) as

$$\alpha(r; R) = 1 - \frac{3}{4}\frac{r}{R} + \frac{1}{16}\left(\frac{r}{R}\right)^3 = \left(1 - \frac{r}{2R}\right)^2\left(1 + \frac{r}{4R}\right) \quad \text{if } r \leq 2R \qquad (9)$$

and zero if $r > 2R$. This is just the shape function that is widely used in describing scattering from spherical micro-crystallites (see, for example, Lei *et al.*, 2009), but is used in quite a different context here, as it is merely an arbitrary but convenient sampling volume. Using the real-space pair density $\rho(r)$ to convert the sum in (8) into an integral, we can write

$$\frac{\langle N(R)^2\rangle - \langle N(R)\rangle^2}{\langle N(R)\rangle} = 1 - \rho_0 \frac{4\pi}{3} R^3 + \int_0^\infty 4\pi r^2 \rho(r)\alpha(r; R)\,\mathrm{d}r. \qquad (10)$$

Using the identity

$$\rho_0 \frac{4\pi}{3} R^3 = \rho_0 \int_0^\infty 4\pi r^2 \alpha(r; R)\,\mathrm{d}r \qquad (11)$$

we obtain the following result,

$$\frac{\langle N(R)^2\rangle - \langle N(R)\rangle^2}{\langle N(R)\rangle} = 1 + \int_0^\infty 4\pi r^2 [\rho(r) - \rho_0]\alpha(r; R)\,\mathrm{d}r \qquad (12)$$

which can be conveniently re-written as

$$\frac{\langle N(R)^2\rangle - \langle N(R)\rangle^2}{\langle N(R)\rangle} = 1 + \int_0^\infty rG(r)\alpha(r; R)\,\mathrm{d}r. \qquad (13)$$

Comparing (13) with (7), they are clearly equivalent as $R \rightarrow \infty$, because the integrand in (13) contains $\alpha(r; R)$ which tends to unity for all r as $R \rightarrow \infty$. The presence of $\alpha(r; R)$ arises due to the finite nature of the sampling volume, and acts as a natural convergence factor for the integral in (7). Note that the relative variance of $N(R)$ is not related to $S(Q)$ except in the limit as both $R \rightarrow \infty$ and $Q \rightarrow 0$. The sampling volume factor $\alpha(r; R)$ for a sphere can be written as a Taylor expansion in integer powers of $1/R$, allowing the relative variance to be written in the form

$$\frac{\langle N(R)^2\rangle - \langle N(R)\rangle^2}{\langle N(R)\rangle} = a + b/R + O(1/R^3), \qquad (14)$$

where $a = S(0)$ is the desired result and b describes the surface dependence associated with the sampling volume. In conjunction with (2), equation (14) is therefore a simple but exact relation that allows one to obtain the structure factor $S(Q \rightarrow 0)$ from a large model structure contained within a super-cell that periodically repeats, and avoids problems associated with extrapolating an oscillating function. We have found this to be the best possible procedure.

The use of the shape function as a convergence factor, as seen in (13), can be generalized to all values of Q. By inserting the shape function into the integrand of (1) and solving for $S(Q)$, one obtains

$$\begin{aligned} S(Q) &= 1 + \int_0^\infty 4\pi r^2 [\rho(r) - \rho_0](\sin Qr/Qr)\alpha(r; R)\,\mathrm{d}r \\ &= 1 + \int_0^\infty rG(r)(\sin Qr/Qr)\alpha(r; R)\,\mathrm{d}r. \end{aligned} \qquad (15)$$

The limiting result as $R \rightarrow \infty$ can be estimated from an extrapolation by the same technique as for the $Q \rightarrow 0$ case previously discussed. The advantage of using (15) over (1) and (6) is that the added convergence factor removes the oscillations in $S(Q)$ that are artefacts of the finite size of the model and gives good results at all Q.

3. Results

3.1. Amorphous silicon

One major focus of this paper is to determine the limit $S(Q \rightarrow 0)$ for amorphous silicon from computer models which serves as a prediction for this important material. As discussed earlier, there is more than one way to find the limit $S(Q \rightarrow 0)$, and we will explain the numerical results obtained from all of them here.

The first approach is shown in Fig. 1, where we show the most direct calculation of $S(Q)$ using (6) at the points $Q_{lmn} = (2\pi/L)(l^2 + m^2 + n^2)^{1/2}$ determined by the super-cell. While this gives a good overall description of $S(Q)$, it is very limited at small Q and extrapolation or analytic continuation to $Q = 0$ is not possible, even for the much larger 100K model. This is because the finite size oscillations are too severe. At small Q, the scattering is just the shape factor of a spherically averaged cube (Lei *et al.*, 2009; Goodisman, 1980; Goodisman & Coppa, 1981; Kodama *et al.*, 2006). Note that the higher density of the 100K model leads to a shift of the peaks to slightly larger Q values. Note also that the structure factor approaches unity at large Q as it must, which sets the scale for comparison for the limit $S(Q \rightarrow 0)$. No harmonic phonons (or zero-point motion *etc.*) were added to any of the results in this paper. The inclusion of harmonic phonons would have the effect of

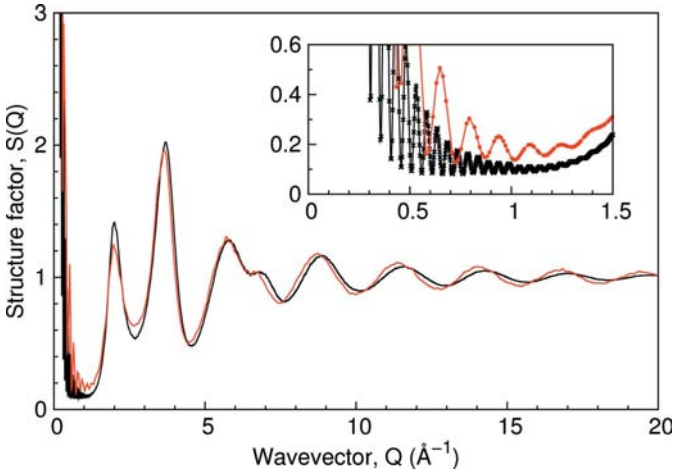

Figure 1
The structure factor for amorphous silicon is calculated directly using equation (6) at the super-cell values Q_{lmn}, shown in the inset as red circles for the 4096 atom model and black crosses for the 100K model.

adding a term that goes as Q^2 at small Q, but this would vanish as $Q \rightarrow 0$.

The second method is the Fourier transform method in which $S(Q)$ is determined from the sine transform using (1) with $G(r)$ input from the model. Both models of amorphous silicon, containing 4096 and 100K atoms, are used in Fig. 2 which shows the distribution $G(r) = 4\pi r[\rho(r) - \rho_0]$. Note the differences in the two silicon models. The difference of 5% in the densities is apparent at small r where $G(r) = -4\pi r\rho_0$, and by the small shift in the peak positions. For comparison, the average separation of bonded silicon atoms determined from the first peak is 2.35 Å in the 4096 atom model but only 2.31 Å in the 100K model. An isotropic contraction of the whole system does not affect the limit $S(Q \rightarrow 0)$, so to first order the overly dense 100K model should give appropriate values in the limit, as there is no length metric in the limit $Q \rightarrow 0$.

The structure factor can be found by applying (1) using $G(r)$ for each model. Only the structure factor of the 100K model is

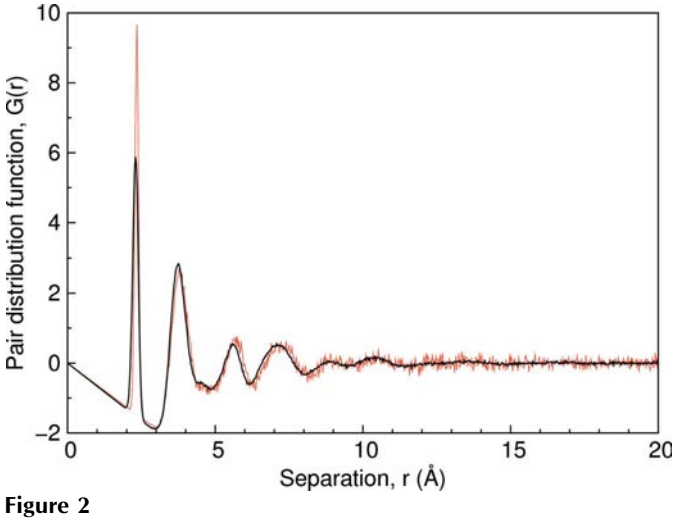

Figure 2
The pair distribution function $G(r)$ for amorphous silicon for the 4096 atom model (rough red line) and the 100K model (smooth black line).

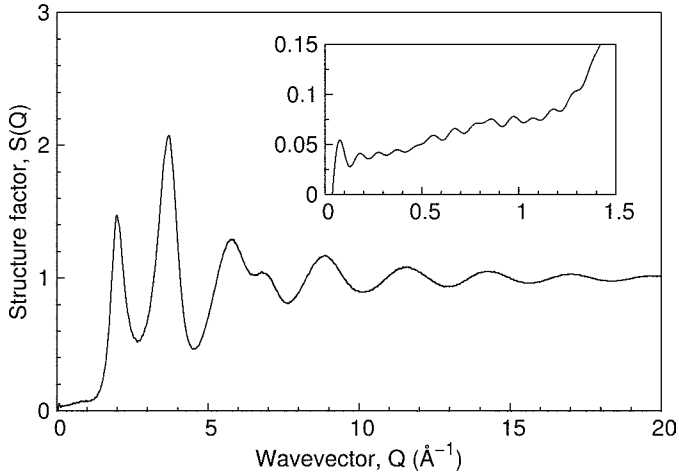

Figure 3
The structure factor $S(Q)$ for amorphous silicon obtained from equation (1) for the 100K model. The inset shows the small Q region expanded.

shown in Fig. 3, where even here the difficulty of trying to extrapolate to $Q = 0$ is again apparent, although the situation is improved somewhat from the direct method shown in Fig. 1.

From the inset of Fig. 3 that displays $S(Q)$ at small Q, the structure factor of the 100K model still shows significant but reduced oscillations owing to finite size effects. Of course these oscillations are even more pronounced for the 4096 atom model, which is not shown. Here $G(r)$ is truncated beyond $L/2$ (half the width of the cubic super-cell), beyond which $G(r)$ is almost but not quite zero. The source of the oscillations is apparent from their wavelength of $2\pi/(L/2)$, and is reduced in amplitude compared with those in Fig. 1, because all Q values over a sphere are taken into account and not just the Q_{lmn}. A very approximate limit of $S(Q \rightarrow 0) \cong 0.03$ can be extrapolated by eye for the 100K model from Fig. 3, through the ripples in the inset, but the uncertainty is almost as large as the value itself. For the smaller 4096 atom model, the oscillations are even larger, making any attempt to extrapolate $S(Q)$ quite hopeless. Smoothing techniques can be used to attenuate the oscillations, but they are not very convincing. There is a better approach.

An alternative to the Fourier transform approach derived in §2.3 involves finding the relative variance within finite sampling volumes of increasing size (but identical shape; we have used spheres) and extrapolating to the thermodynamic limit. This has the great operational advantage of avoiding oscillations. The relative variance in the number of atoms within spheres of different radii is plotted in Fig. 4 for both silicon models. The distribution $G(r)$ can only be computed safely out to $r = L/2$ owing to the periodic nature of the model. As the sampling volume factor $\alpha(r; R)$ for a sphere is non-zero out to $r = 2R$, the relative variance should only be computed using (13) for $R \leq L/4$, causing the curve for the 4096 model to terminate at a larger value of $1/R = 4/L$ than that for the 100K model. The relative variance for the 100K model shows a definite linear region within the interval 12 Å $< R <$ 20 Å or 0.05 Å^{-1} $< 1/R <$ 0.083 Å^{-1}. From Fig. 2, the lower limit

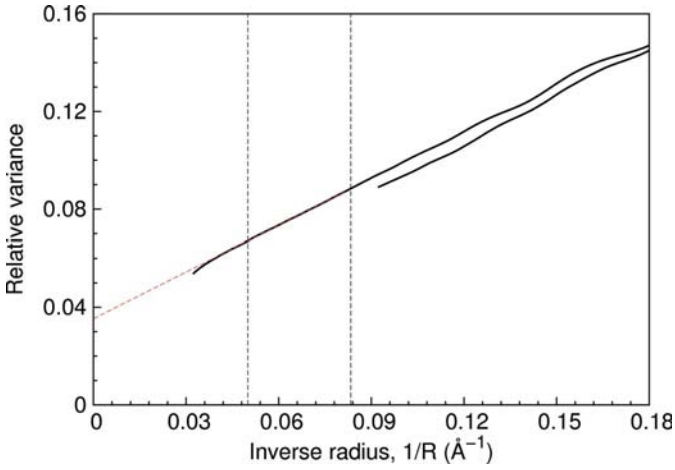

Figure 4
The relative variance in the number fluctuations in amorphous silicon is computed within spheres of various radii R using the sampling volume method. The extrapolated value, shown in red, of $S(0)$, which is just the limit of the relative variance for small $1/R$, is given by $S(Q \rightarrow 0) = 0.035 \pm 0.001$ for the 100K model using equation (14). The vertical dashed lines indicate the range over which the linear fit was performed. It can be seen that the smallest value of $1/R$ for the 4096 atom model is larger than the upper limit of the range over which the relative variance is sufficiently linear and therefore reliable extrapolation would be difficult.

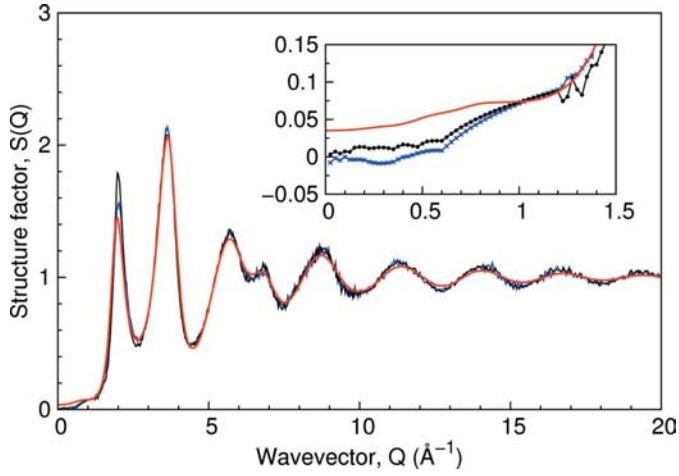

Figure 5
Comparison of the structure factor for amorphous silicon (as implanted, blue crosses, and annealed, black circles) experimentally determined by Laaziri *et al.* (1999*b*) with the structure factor for the 100K model (red curve, no points), rescaled to make the density of the model match that of crystalline silicon and hence void-free amorphous silicon.

$R_{\rm min}$ = 12 Å corresponds to the distance at which strong correlations in atom pair separations all but vanish. The upper limit $R_{\rm max}$ = 20 Å corresponds to the radius at which the relative variance within the spherical volumes begins to deviate noticeably from its linear behavior owing to the finite size of the periodic model (Salacuse *et al.*, 1996). For the 100K model, the maximum possible radius given the sampling volume argument above is $L/4$ = 31 Å, so 20 Å $\simeq L/6$ represents a conservative and safe cut-off. If the largest sampling volume for which the relative variance maintains linear behavior is assumed to be determined by the ratio of the width of the sampling volume to the width of the model, we would expect the linear region to be entirely absent for the 4096 atom model, as $R_{\rm max} = L/6 \cong 7.2$ Å is less than the lower limit $R_{\rm min}$ = 12 Å. Indeed this is what is observed in Fig. 4 for the 4096 atom model, as the oscillations at large values of $1/R$ are still significant by the time the lower limit of $4/L$ is reached. These observations would imply that there is a critical size that a model should be in order for a good extrapolation to $S(Q \rightarrow 0)$ in the thermodynamic limit to be possible. At a minimum, the width of the box (or, for general shapes, the minimum diameter) should be greater than six times the distance over which strong correlations in atomic pair separations persist in order for a linear fitting window to exist. For amorphous silicon, this bare minimum would correspond to a periodic super-cell with sides of length 70 Å containing ∼18 000 atoms. To obtain a window of decent size for the linear fit, it would be very difficult to work with a model of less than ∼50 000 atoms.

The value of the limit $S(Q \rightarrow 0)$ found from linear extrapolation over the linear region of the 100K model is $S(Q \rightarrow 0) = 0.035 \pm 0.001$, where the uncertainty represents the spread in the values of the intercept that result for slightly different choices of the fitting interval. Applying the same extrapolation technique for all Q values, according to (15), results in a structure factor similar to that of Fig. 3 but without the oscillations due to the finite size of the model, as shown in Fig. 5. The large Q values are unaffected by using the convergence factor in (15), but there is a significant effect at small values of Q.

In order to compare with experiment, the Q values of the structure factor for the 100K model shown in Fig. 5 were decreased to 0.985 of their original value to account for the fact that the model has a higher density than that of crystalline silicon and hence void-free amorphous silicon. The rescaled structure factor shows good agreement with the experimental results of Laaziri *et al.* (1999*b*) (whom we thank for providing original data points used in Fig. 5) except for differences in the low Q region and in the amplitude of the oscillations. This requires further modeling to determine the effects of the angular spread at the silicon atom, ring statistics *etc.* on the structure factor.

3.2. Vitreous silica model

The behavior of density fluctuations for the 100K model of amorphous silicon can be compared with the large model of vitreous silica (300K model) produced by Vink & Barkema (2003).

In general for polyatomic systems, it is useful to define partial pair distribution functions (PPDFs) and their corresponding Faber–Ziman partial structure factors (Faber & Ziman, 1965). For vitreous SiO_2, the three PPDFs are $G_{\rm SiSi}(r)$, $G_{\rm OO}(r)$ and $G_{\rm SiO}(r)$, where the PPDFs are computed using the subsets of atom types specified by their respective subscripts.

Fig. 6 displays the PPDF $G_{\rm SiSi}(r)$ superimposed on $G(r)$ from the 100K silicon model, where the silicon distances in the 300K model have been decreased by a factor of 1.33 to make the silicon atom densities the same.

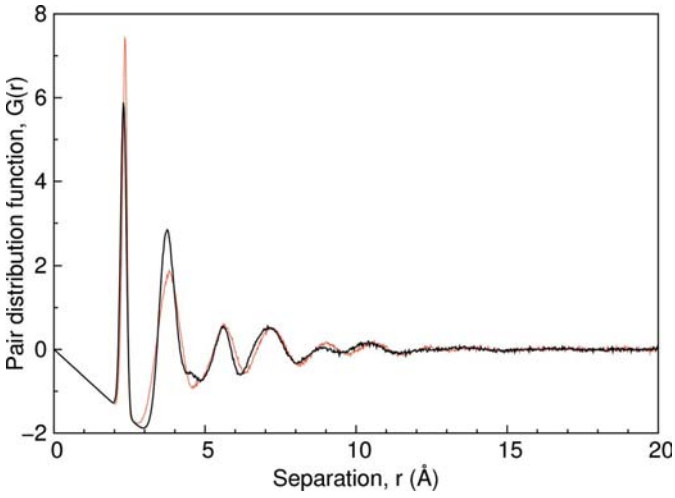

Figure 6
The pair distribution function $G_{\rm SiSi}(r)$ for the 300K vitreous silica model (thin red line) rescaled by a length factor of 1/1.33 and superimposed on the same distribution from the 100K amorphous silicon model (thick black line, as in Fig. 2).

Of course the two distributions are not the same, nor should they be, but are quite surprisingly close. Using the rescaled PPDF $G_{\rm SiSi}(r)$ of vitreous silica as an example of a distorted model for amorphous silicon leads to $S_{\rm SiSi}(Q \rightarrow 0) = 0.039 \pm 0.001$ by applying the sampling volume method, and is close to the value of $S_{\rm SiSi}(Q \rightarrow 0) = 0.035 \pm 0.001$ for the 100K model obtained in the previous section. Thus it appears that the fourfold tetrahedral coordination of the amorphous network may be the most important factor in determining $S(Q \rightarrow 0)$ for amorphous silicon.

The three associated Faber–Ziman partial structure factors (for which primed notation will henceforth be used) $S'_{\rm SiSi}(r)$, $S'_{\rm OO}(r)$ and $S'_{\rm SiO}(r)$ can be found from their respective PPDFs through the sine Fourier transform (Salmon, 2007)

$$Q\big[S'_{\alpha\beta}(Q) - 1\big] = \rho_o \int_0^\infty 4\pi r\big[g_{\alpha\beta}(r) - 1\big] \sin Qr \, {\rm d}r, \qquad (16)$$

where ρ_o is the number density associated with all the atoms in the system, $g(r)$ is the reduced pair distribution function [a scaled version of $\rho(r)$ such that it oscillates about unity at large r], and α and β define the atom pairs used in the distribution function. This definition of the partial structure factor differs from the intuitive definition that would be obtained if atoms of each type were treated in isolation. This more intuitive definition (for which we use unprimed notation) is represented by partial structure factors of the form

$$Q\big[S_{\alpha\alpha}(Q) - 1\big] = \rho_\alpha \int_0^\infty 4\pi r\big[g_{\alpha\alpha}(r) - 1\big] \sin Qr \, {\rm d}r, \qquad (17)$$

where ρ_α is the number density of atoms of type α. These two distributions are simply related by

$$S_{\alpha\alpha}(Q) - 1 = (\rho_\alpha \rho_o)\big[S'_{\alpha\alpha}(Q) - 1\big] = c_\alpha\big[S'_{\alpha\alpha}(Q) - 1\big], \qquad (18)$$

where $c_\alpha = \rho_\alpha/\rho_o$ is the fraction of atoms of type α. Three Bhatia–Thornton structure factors (Bhatia & Thornton, 1970; Salmon, 2006, 2007; Fischer *et al.*, 2006) that describe correlations between atom number and concentration can be defined in terms of the three $S'_{\alpha\beta}(Q)$ according to

$$S_{NN}(Q) = c_{\rm Si}^2 S'_{\rm SiSi}(Q) + c_{\rm O}^2 S'_{\rm OO}(Q) + 2c_{\rm Si}c_{\rm O}S'_{\rm SiO}(Q), \qquad (19a)$$

$$S_{cc}(Q) = c_{\rm Si}c_{\rm O}\big\{1 + c_{\rm Si}c_{\rm O}\big[S'_{\rm SiSi}(Q) + S'_{\rm OO}(Q) - 2S'_{\rm SiO}(Q)\big]\big\}, \qquad (19b)$$

$$S_{Nc}(Q) = c_{\rm Si}c_{\rm O}\big\{c_{\rm Si}\big[S'_{\rm SiSi}(Q) - S'_{\rm SiO}(Q)\big] - c_{\rm O}\big[S'_{\rm OO}(Q) - S'_{\rm SiO}(Q)\big]\big\}. \qquad (19c)$$

Three of the six unknowns in (19) can be found in the limit as $Q \rightarrow 0$ by applying the sampling volume method [equation (13)] to $G_{\rm SiSi}(r)$, $G_{\rm OO}(r)$ and $G_{NN}(r)$ [avoiding terms of type $G_{\alpha\beta}(r)$ with $\alpha \neq \beta$]. It should be noted that the pair of functions $G_{NN}(r)$ and $S_{NN}(Q)$ weight all atoms equally, causing $S_{NN}(Q)$ to differ from the total structure factor for materials with atoms of more than one scattering length. The fitting interval inside of which the relative variance is linear in $1/R$ was found to be 13 Å $< R <$ 19 Å, where 19 Å $\simeq L/9$ is more strict than the limit found for the 100K model of amorphous silicon, suggesting the necessity for an even larger model than the 100K in order to make an accurate estimate of the limit $S(Q \rightarrow 0)$. Fitting within this interval results in the limiting values $S_{\rm SiSi}(Q \rightarrow 0) = 0.039 \pm 0.001$, $S_{\rm OO}(Q \rightarrow 0) = 0.078 \pm 0.002$ and $S_{NN}(Q \rightarrow 0) = 0.116 \pm 0.003$, as shown in Fig. 7. Inserting these values into the three Bhatia–Thornton relations [equations (19)] and solving for the remaining three unknowns, one finds $S_{\rm SiO}(Q \rightarrow 0) = 0.116$, $S_{cc}(Q \rightarrow 0) = -1.5 \times 10^{-5}$ and $S_{Nc}(Q \rightarrow 0) = 1.0 \times 10^{-5}$. Within the uncertainty of the extrapolation, and remembering that there are $\sim 10^5$ atoms in the model, the limits of the last two Bhatia–Thornton structure factors are consistent with zero, *i.e.* $S_{cc}(Q \rightarrow 0) = S_{Nc}(Q \rightarrow 0) = 0$. This reflects the fact that the chemical disorder is virtually zero, as only several out of the 100 000 silicon atoms in the model are bonded to another silicon atom instead of to an oxygen atom.

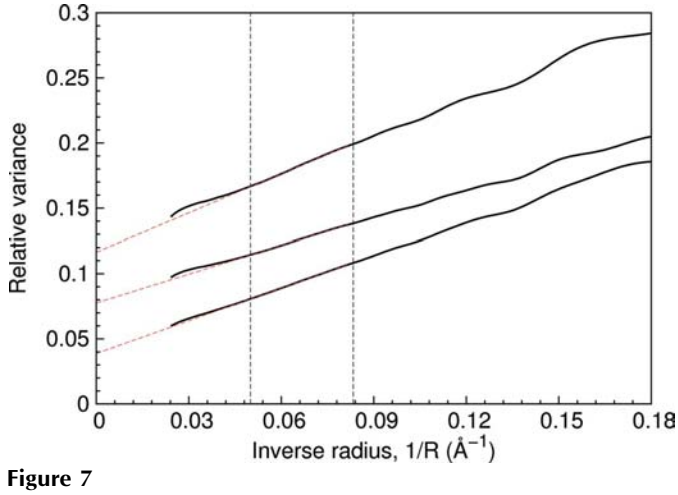

Figure 7
The relative variance of the number fluctuations in vitreous silica within sampling spheres of radii R. The variance is computed using the sampling volume method and plotted against $1/R$. The extrapolated values, shown in red, are given by $S_{\rm SiSi}(Q \rightarrow 0) = 0.039 \pm 0.001$, $S_{\rm OO}(Q \rightarrow 0) = 0.078 \pm 0.002$ and $S_{NN}(Q \rightarrow 0) = 0.116 \pm 0.003$.

If the two quantities $S_{cc}(Q \to 0)$ and $S_{Nc}(Q \to 0)$ are exactly zero, which we will take to be true from now on, the relationship between the limiting values of the other structure factors simplify greatly, and can all be expressed in terms of a single structure factor rather than the original three. Equations (19*a*)–(19*c*) can be rewritten as

$$S'_{\mathrm{SiSi}}(Q \to 0) = S_{NN}(Q \to 0) - \left(c_{\mathrm{O}}/c_{\mathrm{Si}}\right), \quad (20a)$$

$$S'_{\mathrm{OO}}(Q \to 0) = S_{NN}(Q \to 0) - \left(c_{\mathrm{Si}}/c_{\mathrm{O}}\right), \quad (20b)$$

$$S'_{\mathrm{SiO}}(Q \to 0) = S_{NN}(Q \to 0) + 1. \quad (20c)$$

From (18), one can write down the relations

$$S'_{\mathrm{SiSi}}(Q) = \left(1/c_{\mathrm{Si}}\right)S_{\mathrm{SiSi}}(Q) - \left(c_{\mathrm{O}}/c_{\mathrm{Si}}\right), \quad (21a)$$

$$S'_{\mathrm{OO}}(Q) = \left(1/c_{\mathrm{O}}\right)S_{\mathrm{OO}}(Q) - \left(c_{\mathrm{Si}}/c_{\mathrm{O}}\right). \quad (21b)$$

In the thermodynamic limit, the previous five equations relate the limiting values of the six structure factors, and thus there is only one independent quantity. If the independent quantity is chosen to be $S_{NN}(0)$, the limiting values of the other structure factors that one would find if each atom type was taken in isolation can be expressed in terms of the Bhatia–Thornton number correlation $S_{NN}(0)$ as

$$S_{\mathrm{SiSi}}(Q \to 0) = c_{\mathrm{Si}}S_{NN}(0), \quad (22a)$$

$$S_{\mathrm{OO}}(Q \to 0) = c_{\mathrm{O}}S_{NN}(0). \quad (22b)$$

The scaling factors that exist between these three values when there is no chemical disorder in the system explains why the values found from the sampling volume method follow a 1:2:3 ratio [$S_{\mathrm{SiSi}}(Q \to 0) = 0.039 \pm 0.001$, $S_{\mathrm{OO}}(Q \to 0) = 0.078 \pm 0.002$ and $S_{NN}(Q \to 0) = 0.116 \pm 0.003$], as $c_{\mathrm{Si}} = 1/3$ and $c_{\mathrm{Si}} = 2/3$. Note that this scaling is only present as $Q \to 0$ and of course is not true for general values of Q. All the analysis of the 300K vitreous silica model can therefore be summarized in a single number by there being virtually no chemical disorder and $S_{NN}(Q \to 0) = 0.116 \pm 0.003$.

The expression for the limiting value of the differential scattering cross section per atom obtained from scattering experiments also simplifies if no chemical disorder is present. The general form of the differential cross section per atom (Fischer *et al.*, 2006; Salmon, 2006, 2007), namely

$$\sum_{\alpha\beta} c_\alpha c_\beta b_\alpha b_\beta \left[S'_{\alpha\beta}(Q) - 1\right] + \sum_\alpha c_\alpha b_\alpha^2, \quad (23)$$

where b_α is the scattering length of atoms of type α, can be simplified in the limit $Q \to 0$ by writing the three Faber–Ziman partial structure factors $S'_{\mathrm{SiSi}}(Q \to 0)$, $S'_{\mathrm{OO}}(Q \to 0)$ and $S'_{\mathrm{SiO}}(Q \to 0)$ in (23) in terms of $S_{NN}(Q \to 0) = S(0)$ using equations (21) and (22). Performing the substitutions, one finds that the $Q \to 0$ limit of the differential cross section per atom simplifies to

$$\left(c_{\mathrm{Si}}b_{\mathrm{Si}} + c_{\mathrm{O}}b_{\mathrm{O}}\right)^2 S(0). \quad (24)$$

Equation (24) is often used to interpret experimental data (Levelut *et al.*, 2002, 2005, 2007; Wright *et al.*, 2005; Wright, 2008) under the assumption that the AX_2 units can be considered as the basic entity, with an associated scattering factor $(c_{\mathrm{Si}}b_{\mathrm{Si}} + c_{\mathrm{O}}b_{\mathrm{O}})$. It was not clear to us until doing the present analysis that this was justified, as two out of the four neighboring oxygen atoms are arbitrarily associated with a silicon atom, and, in addition, this SiO_2 unit may straddle the perimeter of the sampling volume, leading to partial counting. Nevertheless, the above derivation shows that this widely used phenomenological assumption [equation (24)] is indeed justified and correct, subject to there being no chemical concentration fluctuations, so that each silicon atom is bonded to four oxygen atoms and each oxygen atom is bonded to two silicon atoms.

Experiments to determine the absolute value of $S(0)$ are not easy because the scattering has to be normalized to a standard, and also because of multiple-scattering corrections that are best determined by performing measurements on a number of samples of varying thickness and extrapolating to zero thickness. This complicated procedure has been carried out recently by Wright (Wright *et al.*, 2005; Wright, 2008) who, using equation (24), obtains a value for vitreous silica of 0.0300 ± 0.0016 per formula unit, which by incorporating the factor of three (the number of atoms per chemical group) leads to a value for the structure factor of $S(0) = 0.0900 \pm 0.0048$. Note that Wright was able to get down to $Q \simeq 0.02$ Å^{-1}, which is about a factor of ten better than can be obtained with the 300K model. The model value of $S(0) = 0.116$ is about 20% higher than the experimental value, which we comment on below. Nevertheless, this is the first calculation of $S(0)$ from a model of vitreous silica and is gratifyingly close to the experimental value. The density of the vitreous silica sample (Wright *et al.*, 2005; Wright, 2008) and the model are the same to within 0.1%.

We note that Salmon (Salmon, 2006, 2007; Salmon *et al.*, 2007) has made measurements of structure factors on a number of AX_2 glasses using isotopes so that the partial structure factors can be found, and hence $S_{NN}(Q)$. These experiments are a real *tour de force* but not specifically designed to measure the $Q \to 0$ limit. Measurements were not taken at very small Q (down to $Q \simeq 0.5$ Å^{-1}), but very approximate values can be extrapolated from the plots of the partial structure factors at small Q, giving values between $\sim$0.1 and $\sim$0.15 for GeO_2, $GeSe_2$ and $ZnCl_2$ (Salmon, 2006, 2007; Salmon *et al.*, 2007). These are quite close to the accurate value for vitreous silica obtained by Wright *et al.* and to the model calculation, suggesting *perhaps* that this value, $S(0) \simeq 0.10$, is a general feature of AX_2 glasses, in the same way that a value $S(0) \simeq 0.035$ is characteristic of single-component tetrahedral glasses.

The situation is rather more complex in general (Bhatia & Thornton, 1970), when there is chemical ordering, as equation (4) is generalized to

$$S_{NN}(0) - \delta^2 S_{cc}(0) = \rho_0 k_{\mathrm{B}} T \chi_T, \quad (25)$$

where δ is a size difference factor associated with the two types of atoms, and gives the (usually small) second term in (25). In vitreous silica, this term involving δ is zero because $S_{cc}(0) = 0$. It is expected to also be very small in the liquid phase and so we will ignore it in the comments in the next section.

4. Comments

For an ergodic system in thermal equilibrium, like a liquid, we expect equation (4) to hold. It is useful to use this relation to assess how far amorphous silicon, as well as other amorphous materials and glasses, are from equilibrium. The compressibility of amorphous silicon is between 2×10^{-11} m^2 N^{-1} and 3×10^{-11} m^2 N^{-1}, obtained from silicon–aluminium alloy data extrapolated to zero aluminium doping (Keita & Steinemann, 1978). Using $\rho_0 = 0.05$ atoms Å^{-3} (Custer *et al.*, 1994; Laaziri *et al.*, 1999*a*), and using a room temperature of 300 K, we find from (4) that $0.004 < S(0) < 0.006$, which is an order of magnitude less than the computer model value of 0.035. If we use the melting temperature of crystalline silicon of roughly $T = 1685$ K (Grimaldi *et al.*, 1991), this estimate increases to $0.023 < S(0) < 0.035$, where we note that both the density ρ_0 and the compressibility χ_T are only weakly temperature dependent so that almost all of the temperature dependence in (4) comes through the temperature factor T itself. Nevertheless, the figures based on high temperatures are in the general area of the value of $S(0) = 0.035$ determined from the 100K model, which is satisfying. Note that the comparison is a little less favorable if we use the melting temperatures of 1220 K to 1420 K for amorphous silicon (Donovan *et al.*, 1989; Grimaldi *et al.*, 1991), which leads to $0.017 < S(0) < 0.030$.

The limiting value $S(Q \rightarrow 0)$ has also been estimated indirectly through measurement of the sound velocity, as discussed by Blairs & Joasoo (1980). The limit $S(Q \rightarrow 0) \simeq 0.0501$ was determined for silicon at a melting temperature of 1685 K, not from a scattering experiment but by applying (4), and using the measured value of the density and the value of the isothermal compressibility determined from the sound velocity. The limit $S(Q \rightarrow 0) = 0.035 \pm 0.001$ found for the 100K model would correspond to an effective fictive temperature of $T_f \simeq 1177$ K; not an unreasonable value for silicon. Note that we have not assigned any temperature dependence to either the density or the compressibility in (4) in determining the effective fictive temperature.

The most extensive and informative data on the structure factor for liquid and vitreous silica has been assembled by Levelut and co-workers (Levelut *et al.*, 2002, 2005, 2007). They have used small-angle X-ray scattering, with wavevectors Q down to ~ 0.027 Å^{-1}, which is comparable with that obtained from the 300K vitreous silica model used in this paper. Absolute measurements are difficult in this region [a notable exception being the work of Wright *et al.* (2005)] and so it was necessary to normalize to the assumed liquid behavior at high temperatures using (4). However, there are discrepancies between compressibility values and so there is some uncertainty as to what values to take (Levelut *et al.*, 2005). Note that there is a factor of $900 = (30)^2$ between the data of Wright and Levelut, owing to the electron units used by Levelut, which in turn differs by a factor of three from the conventional definition of the structure factor as used here and follows Salmon (Fischer *et al.*, 2006; Salmon, 2006, 2007).

To try to gain some perspective, we have used another set of compressibility measurements (Bucaro & Dardy, 1976; Wright *et al.*, 2005; Wright, 2008) and assumed (4) to be true in order to renormalize the Levelut data upward by a factor of 1.43, which is now re-plotted in Fig. 8. This scale factor is the ratio of the liquid compressibility value quoted by Bucaro & Dardy (1976) to the average of the two liquid compressibility values quoted by Levelut *et al.* (2005), *i.e.* $1.43 = 8.50/[(6.16 + 5.69)/2]$.

Fig. 8 raises many interesting questions relating to glass structure and the fictive temperature (Geissberger & Galeener, 1983). It is very plausible from the data of Levelut *et al.* (Levelut *et al.*, 2002; Levelut *et al.*, 2005; Levelut *et al.*, 2007) that the fictive temperature is very close to where the extrapolated straight lines from the glass phase intersect with the liquid structure factor. Note that the temperature dependence is considerably lower in the glass phase and is due to the thermal vibrations about a fixed network topology (Weinberg, 1963; Wright *et al.*, 2005; Wright, 2008). A most important and intriguing question is: how is information about the fictive temperature embedded in the glass at room temperature? Such information presumably involves ring statistics and possibly the oxygen angle distribution, but it is subtle and will require careful modeling to resolve. All models used will have to be as large as those used in this paper to obtain reliable values for $S(0)$, as discussed earlier. The dashed lines drawn through the two isolated points in Fig. 8, parallel to the Levelut *et al.* lines, suggest a fictive temperature of $\sim$1360 K for the Wright sample and an effective fictive temperature of $\sim$1780 K for the 300K vitreous silica model of Vink & Barkema (2003), which is close to the value of 1740 K used for the start of the quench in their computer model. Note that while this close agreement is promising, one must not forget

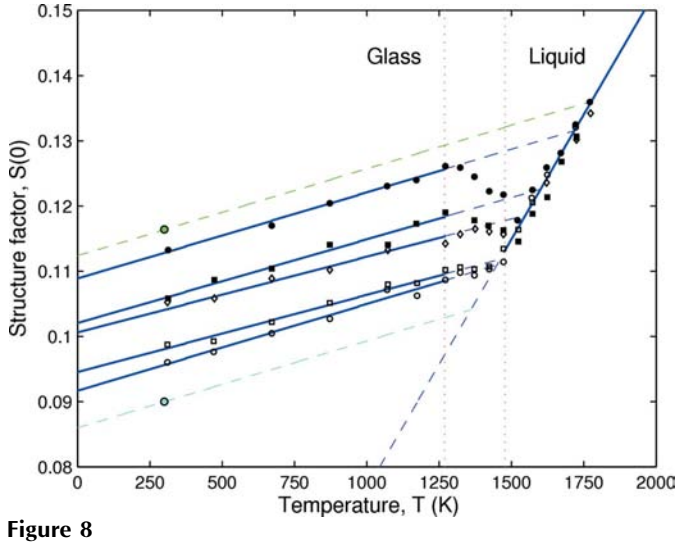

Figure 8
The points and fitted blue solid lines in both the glass and liquid regions of silica are digitized from Fig. 2 of Levelut *et al.* (2005) and multiplied by a factor of 1.43, as described in the text. The five blue lines in the glass phase correspond to fictive temperatures of 1373 K (open circles), 1473 K (open squares), 1533 K (solid squares), 1573 K (open diamonds) and 1773 K (solid circles). The lower isolated point (cyan) is from Wright *et al.* (2005) and the upper isolated point (green) is from the computer model used in this paper. The cyan and green dashed lines are drawn parallel to the solid blue lines to indicate the expected temperature trend and corresponding fictive temperature.

that the computer model is quenched at a much more rapid rate than an actual sample, and it is not clear just how close the values of the experimental fictive temperature and the 'computer' fictive temperature should be. From these results, one might argue that the quench rate is perhaps of secondary importance to the fictive temperature in determining the glass structure, but this is speculative and requires further study.

5. Concluding remarks

The structure factor $S(Q \rightarrow 0)$ for two non-crystalline materials, amorphous silicon and vitreous silica, lies between that of a crystalline solid (where it is close to zero) and that of their respective liquid states. From the computer model of Mousseau, Barkema and Vink, the structure factor for amorphous silicon is computed to be $S(0) = 0.035 \pm 0.001$. This non-zero value is caused by density fluctuations, similar to those found in a liquid, even though the system is far from thermal equilibrium, and seems to be determined largely by the tetrahedral coordination in the amorphous material. This result awaits direct experimental confirmation, when it will also be interesting to measure the temperature dependence, caused by thermal fluctuations about the network structure.

For vitreous silica, the results depend on both the actual temperature and the fictive temperature, as demonstrated clearly by the experimental results of Levelut *et al.* The large periodic computer model of Vink & Barkema gives a reasonable value $S(0) = 0.116 \pm 0.003$ for vitreous silica at room temperature which corresponds to an experimental fictive temperature of about 1780 K, close to 1740 K used computationally to achieve the quenched structure. The intriguing question that remains unanswered is how the information about the fictive temperature is encoded within the network structure, and we speculate that it is in the distinct ring statistics and spread of Si—O—Si angles, but this remains to be demonstrated.

We should like to acknowledge very useful discussions with Austen Angell, Neville Greaves, Gabrielle Long, Simon Moss, Phil Salmon, Adrian Wright and not least Paul Steinhardt, who inspired this work by asking about the structure factor in amorphous silicon in the long-wavelength limit. We also thank Normand Mousseau, Gerard Barkema and Richard Vink for the coordinates of their large amorphous silicon and vitreous silica models, which made this work possible, and Sjoerd Roorda and Simon Moss for the experimental data for amorphous silicon. This work was supported through the FRG grant NSF DMR 0703973.

References

Barkema, G. T. & Mousseau, N. (2000). *Phys. Rev. B*, **62**, 4985–4990.
Bhatia, A. B. & Thornton, D. E. (1970). *Phys. Rev. B*, 3004–3012.
Blairs, S. & Joasoo, U. (1980). *J. Inorg. Nucl. Chem.* **42**, 1555–1558.
Bleher, P. M., Dyson, F. J. & Lebowitz, J. L. (1993). *Phys. Rev. Lett.* **71**, 3047–3050.
Bucaro, J. A. & Dardy, H. D. (1976). *J. Non-Cryst. Solids*, **20**, 149–151.
Custer, J. S., Thompson, M. O., Jacobson, D. C., Poate, J. M., Roorda, S., Sinke, W. C. & Spaepen, F. (1994). *Appl. Phys. Lett.* **64**, 437–439.
Djordjevic, B. R., Thorpe, M. F. & Wooten, F. (1995). *Phys. Rev. B*, **52**, 5685–5689.
Donovan, E. P., Spaepen, F., Poate, J. M. & Jacobson, D. C. (1989). *Appl. Phys. Lett.* **55**, 1516–1518.
Egami, T. & Billinge, S. J. L. (2003). *Underneath the Bragg Peaks: Structural Analysis of Complex Materials*, 1st ed. Amsterdam, Boston: Pergamon.
Faber, T. E. & Ziman, J. M. (1965). *Philos. Mag.* **11**, 153.
Fischer, H. E., Barnes, A. C. & Salmon, P. S. (2006). *Rep. Prog. Phys.* **69**, 233–299.
Geissberger, A. E. & Galeener, F. L. (1983). *Phys. Rev. B*, **28**, 3266–3271.
Goodisman, J. (1980). *J. Appl. Cryst.* **13**, 132–134.
Goodisman, J. & Coppa, N. (1981). *Acta Cryst.* A**37**, 170–180.
Grimaldi, M. G., Baeri, P. & Malvezzi, M. A. (1991). *Phys. Rev. B*, **44**, 1546–1553.
Hansen, J. P. & McDonald, I. R. (1986). *Theory of Simple Liquids*, 2nd. ed. London, New York: Academic.
Keita, N. M. & Steinemann, S. (1978). *J. Phys. C*, **11**, 4635–4641.
Kodama, K., Iikubo, S., Taguchi, T. & Shamoto, S. (2006). *Acta Cryst.* A**62**, 444–453.
Laaziri, K., Kycia, S., Roorda, S., Chicoine, H., Robertson, J. L., Wang, J. & Moss, S. C. (1999*a*). *Phys. Rev. Lett.* **82**, 3460–3463.
Laaziri, K., Kycia, S., Roorda, S., Chicoine, M., Robertson, J. L., Wang, J. & Moss, S. C. (1999*b*). *Phys. Rev. B*, **60**, 13520–13533.
Lei, M., de Graff, A. M. R., Thorpe, M. F., Wells, S. A. & Sartbaeva, A. (2009). *Phys. Rev. B*, **80**, 024118.
Levashov, V. A., Billinge, S. J. L. & Thorpe, M. F. (2005). *Phys. Rev. B*, **72**, 024111.
Levelut, C., Faivre, A., Le Parc, R., Champagnon, B., Hazemann, J. L., David, L., Rochas, C. & Simon, J. P. (2002). *J. Non-Cryst. Solids*, **307**, 426–435.
Levelut, C., Faivre, A., Le Parc, R., Champagnon, B., Hazemann, J. L. & Simon, J. P. (2005). *Phys. Rev. B*, **72**, 224201.
Levelut, C., Le Parc, R., Faivre, A., Brüning, R., Champagnon, B., Martinez, V., Simon, J.-P., Bley, F. & Hazemann, J.-L. (2007). *J. Appl. Cryst.* **40**, s512–s516.
Salacuse, J. J., Denton, A. R. & Egelstaff, P. A. (1996). *Phys. Rev. E*, **53**, 2382–2389.
Salmon, P. S. (2006). *J. Phys. Condens. Matter*, **18**, 11443–11469.
Salmon, P. S. (2007). *J. Phys. Condens. Matter*, **19**, 455208.
Salmon, P. S., Barnes, A. C., Martin, R. A. & Cuello, G. J. (2007). *J. Phys. Condens. Matter*, **19**, 415110.
Sartbaeva, A., Wells, S. A., Treacy, M. M. J. & Thorpe, M. F. (2006). *Nat. Mater.* **5**, 962–965.
Thorpe, M. F. (1983). *J. Non-Cryst. Solids*, **57**, 355–370.
Torquato, S. & Stillinger, F. H. (2003). *Phys. Rev. E*, **68**, 041113.
Vink, R. L. C. & Barkema, G. T. (2003). *Phys. Rev. B*, **67**, 245201.
Vink, R. L. C., Barkema, G. T., Stijnman, M. A. & Bisseling, R. H. (2001). *Phys. Rev. B*, **64**, 245214.
Weinberg, D. L. (1963). *Phys. Lett.* **7**, 324–325.
Wooten, F., Winer, K. & Weaire, D. (1985). *Phys. Rev. Lett.* **54**, 1392–1395.
Wright, A. C. (2008). *Phys. Chem. Glasses*, B**49**, 103–117.
Wright, A. C., Hulme, R. A. & Sinclair, R. N. (2005). *Phys. Chem. Glasses*, **46**, 59–66.